Int J Adv Manuf Technol (2017) 91:2689–2700
DOI 10.1007/s00170-016-9947-8

ORIGINAL ARTICLE

Modeling, design, and implementation of a servo press for metal-forming application

Recep Halicioglu[1] · **L. Canan Dulger**[2] · **A. Tolga Bozdana**[2]

Received: 12 April 2016 / Accepted: 19 December 2016 / Published online: 9 January 2017

Abstract Servo presses have been very popular in engineering applications due to their flexibility, simplicity in construction, and easy control. Many press manufacturer and researchers have studied on servo presses by developing different prototypes. However, only a few models have been commercially available in the market. Servo crank presses can generate different types of motion in their design limitations. They can present wide range of solutions to manufacturers. In this study, a dynamic model is derived by Lagrange approach for a servo crank press machine tool. A load capacity of 50 tons and stroke capacity of 200 mm prototype is designed and manufactured. A new motor-reducer selection methodology is suggested for servo presses. Servo motor-reducer combination is selected. Dynamic model and simulation results are presented with the real system parameters. Experimental validations have been performed on the servo press prototype. System's dynamic model is validated by the experimental results. High precision of the manufactured servo press is also shown.

Keywords Servo press · Dynamic modeling · Machine tool design · Servo motor selection · Metal forming

✉ Recep Halicioglu
rhalicioglu@osmaniye.edu.tr

[1] Department of Mechanical Engineering, University of Osmaniye Korkut Ata, Osmaniye, Turkey

[2] Department of Mechanical Engineering, University of Gaziantep, Gaziantep, Turkey

1 Introduction

Servo presses are the alternatives of conventional and hydraulic presses. They have been used to form sheet and bulk metal for several years. Servo presses exhibit the most remarkable properties of hydraulic and conventional mechanical presses, which can offer flexibility and full tonnage at any time by providing the accuracy and reliability [1, 2]. They have different designs without flywheel, clutch, and brake mechanisms, providing free motion concepts for press applications via servo motor. Although servo presses have been manufactured using different mechanisms, servo crank presses with slider-crank mechanism are the most common type [3–5].

Many studies on design, dynamic modeling, and analysis of slider-crank mechanisms and the crank presses are reported in the literature. Qingyu et al. [6] presented experimental results with motion optimization on a 2500 ton servo press. Comparison of results between the theoretical loading torque and the actual loading torque of motor are given. Fung and Chen [7] have studied dynamic analysis and vibration control of a flexible slider-crank mechanism driven by a permanent magnet (PM) synchronous servo. Geometric constraints for a flexible connecting rod were derived. Ha et al. [8] have derived the dynamic equations of a slider-crank mechanism driven by a servomotor using Hamilton's principle, Lagrange multiplier, geometric constraints, and partitioning method. An identification method based on the real-coded genetic algorithm (RGA) was presented to identify the parameters of the mechanism. Bai et al. [9] have studied ultra-high speed stamping machines (a crank press) and their balancing structure. They have used static mass substitution method for simplicity of analysis, where the Newtonian expressions for dynamic inertia forces were applied. He et al. [10] have presented design, dynamic modeling, and experimental validation of a mechanical metal forming press with two actuators, a

constant speed and a servo motor. The 2-DOF mechanism was controlled by servo motors. The dynamic model of the press was derived by using the kineto-static method. The simulation results were also tested in prototype having a capacity of 250 kN. Li et al. [11, 12] have then studied on hybrid mechanisms are seven-bar and nine-bar presses for deep drawing applications. While kinematic analysis, dynamic analysis, and link optimization has been applied for a seven-bar press mechanism, dynamic modeling of a nine-bar press mechanism has been designed and analyzed. They have used Lagrangian method for dynamic models and have chosen 4th-order Runge Kutta method. Jun [13] has used the basic theory of mechanical dynamics method. Then, kineto-static analysis was used to obtain the numerical solution of slider-crank mechanism. After building the vector model of the slider-crank mechanism, the simulations were compared using MATLAB (Simulink) and ADAMS. Xingguo et al. [14] have designed a virtual prototype of flexible multi-body crankshaft system using ADAMS software for dynamic analysis. Liu et al. [15] have investigated forward kinematic and dynamic analysis of a slider-crank mechanism. Dynamic analysis was modeled by using statical equilibrium (Kineto-static approach). A MATLAB-Simulink model was also built. Daniel and Cavalca [16] have proposed a mathematical model for a slider-crank system by using two models, namely Eksergian Equation of Motion and Lagrange Method. Abdullah and Telegin [17] have presented a dynamic model and its mathematical description of the central slider-crank mechanism for the hot-crank press. Anis [18] has presented kinematic and dynamic analyses of a slider-crank mechanism by using ADAMS with the crank torque of 4.2 Nm and the crank velocity of 6 rad/s with inertias.

Previous studies [6–18] have shown that two types of dynamic analyses were performed; forward and inverse analysis. Lagrangian and kineto-static analysis are used frequently as "dynamic analysis method." MATLAB and ADAMS software have been used.

Related literature is covered considerations of servo press motor selection and application examples. Toyokoki has developed the first commercial servo press 100 kN which is driven by an AC servo motor for accurate bending [19]. Aida DSF-N1 and N2 Straightside series have used AC servo motor [20]. Their tonnage capacities are between 80 and 300 tons, motor capacities are between 25 and 50 kW, and strokes are in the range of 160–400 mm. Andritz Kaiser and Shuler have preferred direct drive systems [21]. Coskunoz also used AC servo motor series for their hybrid press solution [22]. Karakoc KLP Machine group has produced servo knuckle joint presses [23, 24]. They have used high torque series servo motors with capacities of 3.1–325 kW power and 325–32,900 Nm max torque providing the direct-drive technology. Amada has got the servo presses in punching and stamping series. Their AE-NT and EM-NT (direct twist drive) series have capacities of between 20 and 33 tons, and their power requirements are AC 200 V 3-Phase 50/60 Hz and 19–27 kW with 40 mm stroke [25]. Amada has got SDE servo stamping press series [26]. The press capacity is taken as 80–300 tons, and stroke length is between 160 and 400 mm. Stroke speeds change between 80 and 30 strokes per minute (spm), and main motor drives are 25–50 kW. Seyi has developed high electric motor technology, which has low heat generation rate, high heat dissipation efficiency, and 480 V for their SD1–2 servo press series [27]. The servo torque motor capacity is 14,000 Nm (max) and 340 rpm (max). The torque is transferred by means of pinion-main gear (geared direct drive). Komatsu has two series of servo presses that are H2W and H1F [28]. Their capacities are given 38.5–330 tons with strokes changing from 40 to 350 mm. Stroke speeds are between 240 and 50 spm. Their main motor drive power are 5–60 (×2) kW of AC servo motor and torque servo motors. Presses with 50–80-ton capacities are actuated by 15–25 kW AC servo motors. Rated load has been applied at maximum 4–5 mm stroke.

In this study, dynamic modeling of a servo crank press is presented. Dynamic analyses are given by Lagrangian. Motor selection issues are described. The lower power servo motor is provided the higher performance capacity thanks to the suggested selection methodology. A suitable servo motor-reduction unit combination is selected for higher stroke capacity in the rated tonnage by reducing manufacturing cost. A manufactured servo press prototype is operated, and the experimental results are taken. Here, the programmable ram motion is shown experimentally with comments. This study is completed as a part of a research project. The suggested methodology and results in modeling and design steps can provide know how to researchers and industry.

2 System definition and motion details

Servo crank press with a capacity of 50 tons was selected for this study. Figure 1 shows the mechanism's schematic representation. The crank length, the crank angle, the transmission angle, the rod length, the rod angle, and the slider (ram) position are denoted by r, θ, μ, l, β, and y, respectively. TDC indicates the top dead center and BDC indicates the bottom dead center. Besides, r' and l' are the distances of center of gravity of crank (Cg1) and center of gravity of connecting rod (Cg2). The rod-crank ratio is selected as seven to reduce the motion of β. The stroke of mechanism is 200 mm, and hence in-line mechanism's crank length must be 100 mm. The rod length is taken as 700 mm according to crank/rod ratio of 1/7.

The kinematic equations of the crank press system are given in previous studies [3, 4]. The system kinematics is given in Eqs. (1–4) where y is the distance between the crank's center of rotation and the ram position, s represents the press stroke.

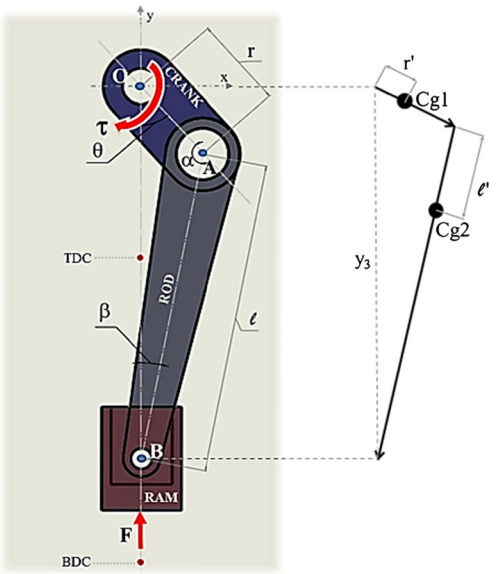

Fig. 1 Design of servo crank press mechanism

Also $\theta, \dot{\theta},$ and $\ddot{\theta}$ are the crank angular position, velocity and acceleration, respectively.

$$s = (l + r) - y \tag{1}$$

$$\theta = \cos^{-1}\left(\frac{r^2 + (r + l - s)^2 - l^2}{2r(r + l - s)}\right) \tag{2}$$

$$\dot{\theta} = \dot{s}\frac{(y^2 - r^2 + 1^2)}{2ry^2\sin\theta} \tag{3}$$

$$\ddot{\theta} = \ddot{s}\frac{(1^2 - r^2 + y^2)}{2ry^2\sin\theta} - \dot{s}^2\frac{(r^2 - 1^2)}{ry^3\sin\theta} - \dot{\theta}^2\frac{\cos\theta}{\sin\theta} \tag{4}$$

2.1 Motion characteristic

The press motion scenario was selected as "soft motion" that it can be obtained only by linkage conventional presses. Figure 2 shows the motion with three parts. There is a quick rise between 0 and 0.5 s: segment 1, while the touching time is very slow (0.5–2.1 s: segment 2). Finally, the return time (2.1–3 s: segment 3) is quickly performed the completing motion in 3 s. The ram position details of the segments are given in Table 1. The motion profile provides smooth surface on formed material in sheet metal-forming process. This scenario is commonly preferred in metal forming industry [5, 22]. The expected reaction force is also shown for characteristic of the ram in Fig. 2. The scenario is based on the most critic motion for deep drawing application and the corresponding force, which is also a requirement for motor selection. Depending on requirements of the user, the scenario can be changed

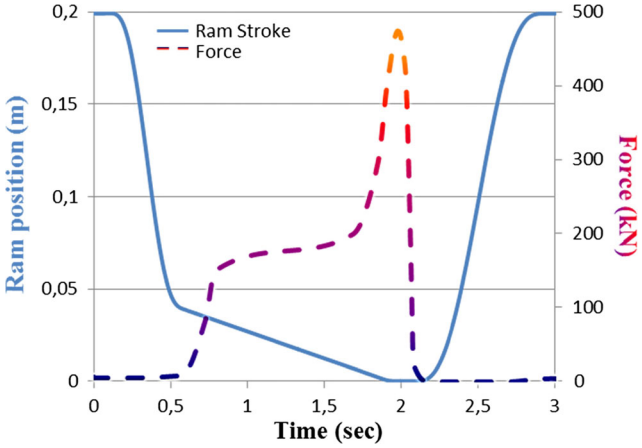

Fig. 2 Ram soft motion and reaction force scenario

yielding different position, velocity, and acceleration values.

3 Dynamic modeling

Dynamic equation of the servo press mechanism is derived by means of Lagrangian. Lagrange's primary contribution is the dependence of kinematical variables on the generalized coordinates. Lagrange method is based on energy expressions with respect to the variables. Lagrangian function states the difference between system kinetic energy and potential energy as in Eq. (5) in which L, T, and V refer to Lagrange function, kinetic energy, and potential energy of system, respectively [29, 30].

$$L = T - V \tag{5}$$

If a set of independent generalized coordinates are considered and the coefficients of δq_k disappear independently for all values of k, then the coefficient is set to zero. General form of Lagrange's equations of motion is given as in Eq. (6), which is also called as Euler-Lagrange equation, where Q_k contains the generalized forces [8].

$$\frac{\mathrm{d}}{\mathrm{d}t}\left(\frac{\mathrm{d}L}{\mathrm{d}\dot{q}_k}\right) - \frac{\mathrm{d}L}{\mathrm{d}q_k} = Q_k, \qquad k = 1, 2, \ldots, n \tag{6}$$

Slider-crank mechanism which is a single-DOF system is given in Fig. 1 where the crank shaft is connected to servo

Table 1 Ram position details of the critic soft motion segments

Segment	Time (s)	Ram position (m)
1	0	0.20
	0.5	0.04
2	0.5	0.04
	2.1	0
3	2.1	0
	3	0.20

motor by a gear unit. The system work is performed by the torque on the crank; the second one is by the force. For the determination of motion and torque graphs, if the losses are ignored, generalized force equations can be written for external forces as given in Appendix Eqs. (26–27).

Detailed system derivations are given in the Appendix and the last form of the system dynamic model is found as in Eq. (7) where τ and F are the crank torque and the ram reaction forces, respectively. Value of c is defined in Appendix as Eq. (25).

$$\begin{aligned}
&\ddot{\theta} r^2 \left(\frac{I_1 + I_2 c^2 + m_1 r'^2}{r^2} + \frac{\left(l - l'\right)^2}{l^2} m_2 \cos^2\theta + \sin^2\theta \left(c^2 \left(\frac{l'^2}{l^2} m_2 + m_3 \right) + 2c \left(\frac{l'}{l} m_2 + m_3 \right) + m_2 + m_3 \right) \right) \\
&+ \frac{\dot{\theta}^2 r^2 \sin^3\theta (c^3 - c)}{\cos\theta} \left(c \left(\frac{I_2}{r^2 \sin^2\theta} + \frac{l'^2}{l^2} m_2 + m_3 \right) + \frac{l'}{l} m_2 + m_3 \right) \\
&+ \dot{\theta}^2 r^2 \sin\theta \cos\theta \left(- \frac{\left(l - l'\right)^2}{l^2} m_2 + c^2 \left(\frac{l'^2}{l^2} m_2 + m_3 \right) + 2c \left(\frac{l'}{l} m_2 + m_3 \right) + m_2 + m_3 \right) \\
&+ gr \sin\theta \left(\frac{r'}{r} m_1 + \frac{l'}{l} m_2 c + m_3 c + m_2 + m_3 \right) \\
&= \tau + \mathrm{Fr} \sin\theta (1 + \mathrm{c})
\end{aligned} \tag{7}$$

4 CAD design

Servo crank press system is generally constructed in two parts: dynamic and static. The dynamic parts are crank + helical gear, pinion shaft + helical gear, and the connecting rod and the ram. C-type mono-block body and its components (welded) are the static parts. The design was started by selection of sleeve bearings since they are the weakest components on the press system. The design was based on methods of machine elements where safety factor was more than two [31]. 3D model of press was built by SolidWorks software® where the mass-inertias were found by the software (Fig. 3). Table 2 gives the mechanical parameters of each part (the crank, the connecting rod, the ram, and other components). The mechanism was considered in line with y direction, and hence the corresponding centers of gravity lengths (CGL) are indicated in Table 2, where the inertias are given in z direction. The mass inertia of the system was found by Eq. (8) on the crank rotational body [32]. This equation is adopted to servo presses and then verified with the experimental studies. The mass inertia of the system reflected to crankshaft was found as 10.55 kg m^2.

$$I_{\mathrm{sys}} = I_1 + m_1 r'^2 + \left(\frac{l - l'}{l} m_2 + \frac{l'}{2l} m_2 + \frac{1}{2} m_3 \right) r^2 \tag{8}$$

5 Simulation results of servo press machine tool

Inverse kinematics is performed by using the system's kinematic expressions given in Eqs. (1–4) in Fig. 2. A motion scenario, soft motion can be seen with the ram velocity, acceleration, and jerk values in Fig. 4a. This profile is preferred in deep drawing applications. The crank angular position, velocity, and acceleration are given in Fig. 4b, where the downward motion of ram and clockwise motion of crank were assumed as negative. Ram stroke acceleration and crank acceleration expressions were derived with the ram jerk. Having performed the kinematics analysis, the system dynamic model in Eq. (7) was derived. The crank torque and power are given in Fig. 5. These kinematic and dynamic results are used for selection of servo motor and gearbox.

6 Servo motor and gearbox selection

In twenty-first century, most motor manufacturers have offered wide range of motors that can be used as servo amplifier or a variable frequency controller. Low speed-high torque servo motors (torque motors) are used for high load applications. Such servomotors allow direct drive alternative on eccentric or crank presses. In 2000s, linear motors were developed although their powers were still limited. Nowadays, AC motor

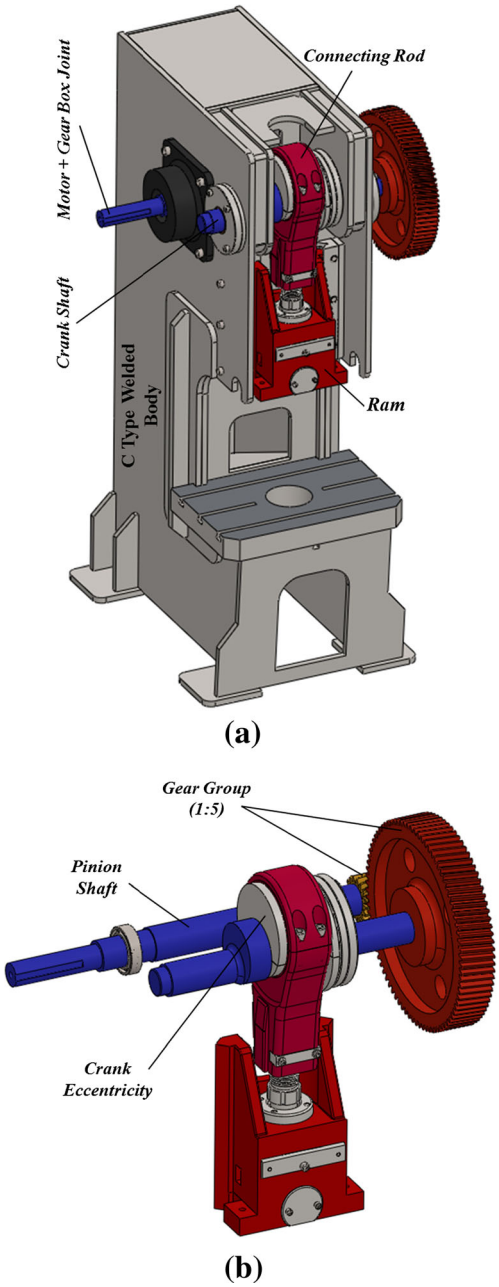

Fig. 3 3D CAD model: **a** complete assembly and **b** transmission mechanism

which can be called as permanent magnet synchronous motor (PMSM) and torque motor technologies are frequently used in servo press industry because of their higher torque capacities [1, 33, 34]. Servo motors can certainly provide flexibility, accuracy, high speed, and high torque. Some factors effecting motor selection are the ambient conditions, the motion profile, the gearbox, the inertia ratio, the load, working cycle, and type of gearbox [35–40].

- *Ambient conditions:* most motors are designed to operate in a maximum ambient temperature of 40 °C.
- *Motion profile:* desired motion profiles with the most critic motions are found via dynamic analysis of the system. The system power is also found by the motion profile as in Eq. (9) in which τ is the torque and w is the angular velocity ($\dot{\theta}$). Motor-rated power capacity (P_r) should always be greater than the system required power (P_s) as given in Eq. (10).

$$P = \tau w \tag{9}$$

$$P_r > P_s \tag{10}$$

- *Gearbox and inertia ratio:* Eq. (11) gives the optimal transmission ratio (gear ratio) for an inertial load. J_L, J_M, and J_g are the optimal load inertia, the motor inertia and the gear inertia, respectively. In the equations, n, w_M, w_L, τ_L, and τ_M are given as the optimal gear ratio, the motor angular velocity, the load angular velocity, the load torque, and the motor torque, respectively. If the system acceleration is high, torque equation must be written related to inertia and acceleration as in Eq. (13). The motor viscous friction coefficient of b and the efficiency of η_g must be considered.

$$n = \sqrt{\frac{J_L + J_g}{J_M}} \tag{11}$$

$$n = \frac{w_M}{w_L} = \frac{\tau_L}{\tau_M \eta_g} \tag{12}$$

$$\tau_M(t) = n\left(J_M + J_g\right)\ddot{\theta}(t) + nb\dot{\theta} + \frac{\tau_L(t)}{n\eta_g} \tag{13}$$

Table 2 Mechanical parameters of the dynamic parts

Parts	Mass (kg)	Inertia (kg m^2)	Length (m)	CGL (m)
Crank shaft + gear	307.70	8.39	r = 0.1	r' = 0.028
Connecting rod	117.59	4.97	l = 0.7	l' = 0.205
Ram	186.30	–	–	–
Pinion shaft + gear	65.02	0.08	–	–

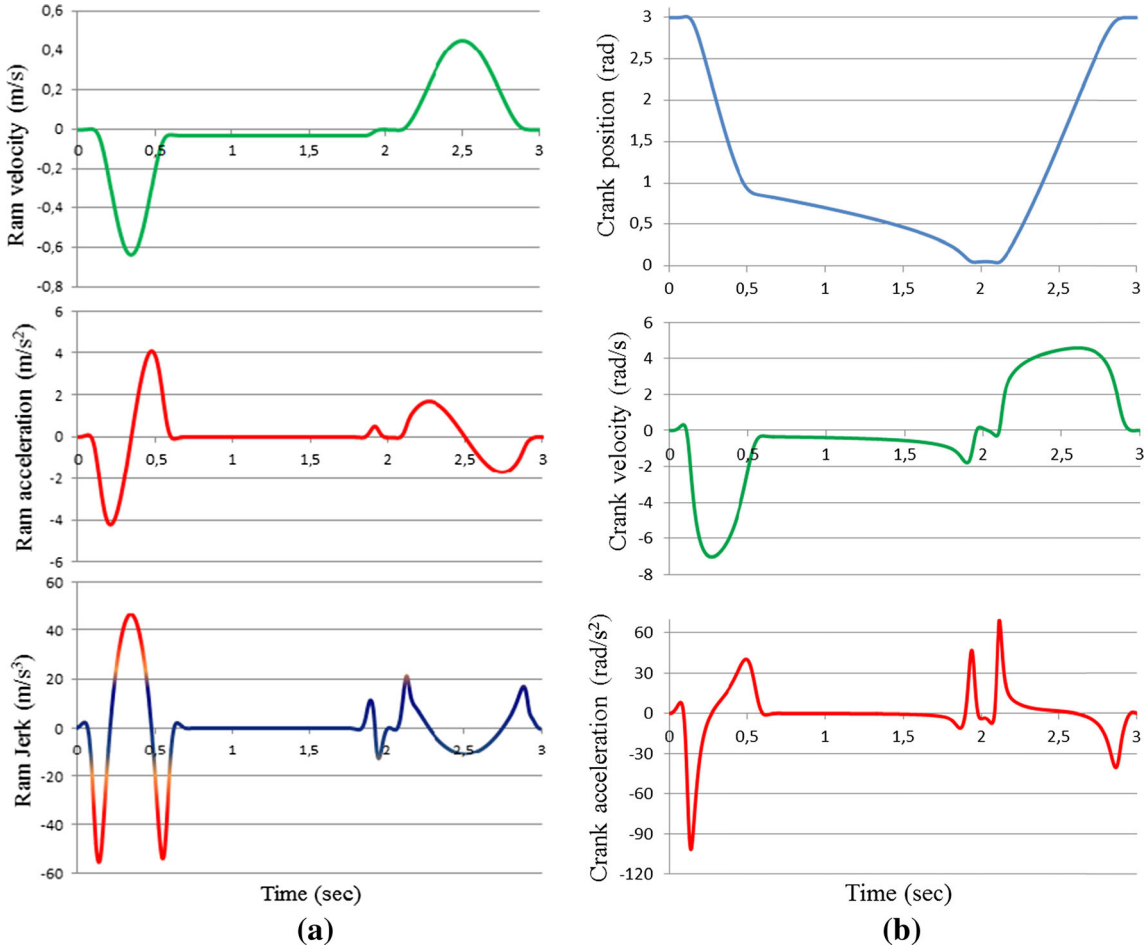

Fig. 4 **a** Ram velocity, acceleration, and jerk and **b** crank position angular velocity and angular acceleration

- *Inertia ratio* (n') is the ratio of the reflected load inertia divided by the motor's rotor inertia, Eq. (14). The reflected inertia (J'_L) is given in Eq. (15). Basic servo drives may require inertia ratios of 3:1 or smaller. High-performance servo drives have auto-tuning, vibration suppression, resonance filters, and disturbance compensation functions that allow up to 30:1 inertia ratios. A ratio between 1:1 and 0.8:1 gives excellent performance, but results in an oversized motor.

$$n' = \frac{J'_L}{J_M} \tag{14}$$

$$J'_L = \frac{J_L}{n^2 \eta_g} + J_g \tag{15}$$

- *Load determination and working cycles:* peak torques (τ_p), rated torques or nominal torque value (τ_r), and root mean square torque (τ_{RMS}) are important parameters during servo motor selection (especially AC servo motors). Calculation of the root mean square (RMS) torque at ideal ambient conditions is given in Eq. (16) where k refers to the number of time deviations in one cycle within period of t_i. The motor must be provided the following relations between the motor (M) and the system (S). The selection of servo motor size (RMS) method is performed.

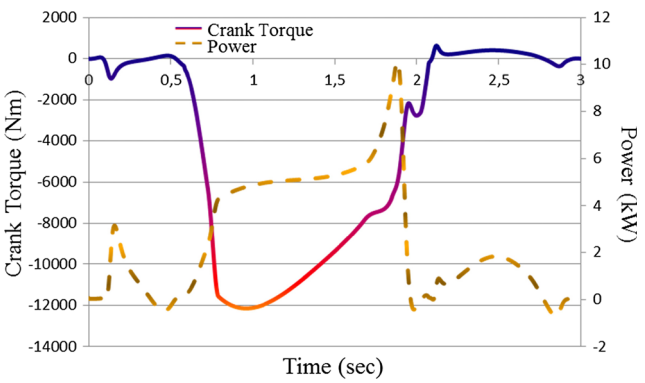

Fig. 5 Crank torque and power

$$\tau_{\mathrm{RMS}} = \sqrt{\sum_{k=1}^{i} {\tau_k}^2 t_k \Big/ t_i} \tag{16}$$

$${\tau_p}^M > {\tau_p}^S, \quad {\tau_{\mathrm{RMS}}}^M > {\tau_{\mathrm{RMS}}}^S \tag{17}$$

- *Selection of servo reducer:* low backlash reducers must be used at servo applications. Some critic parameters are given such as velocity, torque, transmission ratio, service factor, etc. [39–41]. Gearbox output values include the following: the angular velocity (w_G), the torque (τ_G), and the power (P_G) are related to efficiency. Motor outputs and transmission ratio of gear (i) are given in Eqs. (18–20).

$$w_G = w_M \Big/ i \tag{18}$$

$$\tau_G = i\eta_g \tau_M \tag{19}$$

$$P_G = \eta_g P_M \tag{20}$$

6.1 Motor selection for servo press

Servo motors have been extensively used in the last 20 years in many fields such as energy, automotive, manufacturing, and metal forming. Some assumptions and steps should be considered to select a suitable servo motor for 50 tons servo press. The methodology is summarized below:

(1) Ambient conditions were defined. Ambient temperature is lower than 40 °C.
(2) As the motor capacity is quite high, servo PMSM with 400 V and three-phase capacity was selected.
(3) Servo press's crank motion profiles and crank load were readily obtained by the dynamic analysis as given Figs. 4 and 5. They give the maximum values on the crank shaft, which are velocity, torque, and power as about 7 rad/s (67 rpm), 12,100 Nm, and 10 kW, respectively.
(4) The ratio between pinion and crank helical gears is 1:5 with 96% efficiency as given in Fig. 3. Crank values are reflected to the pinion shaft as in Eq. (12). Pinion maximum velocity, torque, and power were found as 335 rpm, 2521 Nm, and 10.42 kW, respectively.
(5) If torque factor of 1.5 is used for higher value of forces, pinion torque and power are found as 3782 Nm and 15 kW. These values were taken for motor + gear box selection constrains. Motor maximum values must be over these values y using Eqs. (18–20).
(6) Reflected inertia on the pinion shaft can be found by Eq. (21). I_{sys} is the reflected inertia on crank shaft that is found by Eq. (8) with Table 2. The reflected inertia on the pinion shaft is found as 0.519 kg m^2.

$$J_L = \frac{I_{sys}}{n^2 \eta_g} + I_{psh} \tag{21}$$

(7) Parker M_2053090 400VAC servo motor® was chosen at the end. Table 3 gives the motor's properties [42]. S3 (400 V) working cycle is considered for the maximum values.
(8) Motion transmission between the actuator and load is defined. Pinion maximum velocity and maximum torque are 335 rpm and 3782 Nm, respectively. The candidate motor's maximum torques is searched on the catalogs based on Eq. (19). If 1:10 gearbox transmission ratio is used in Eq. (19) with the gear box efficiency of 96%, then 3782 Nm of torque can be generated by the motor as the maximum peak torque of motor is 400 Nm. The motor's peak torques can reach about 4000 Nm as reflected to pinion via 1:10 gear box. Also, necessary maximum velocity for this system was calculated as 3350 rpm by Eq. (18) that is suitable for the motor. Since the values are suitable in S3 cycle for this study, transmission ratio between motor and crank was considered as 1:50. Necessary power was calculated as 16.28 kW by Eq. (20).
(9) The reducer type and the ratio are defined. Selected reducer's maximum input and output torques and velocity values can provide the desired parameters.
(10) A suitable reducer was selected as SEW's reduced backlash helical bevel gear unit® with servo adopter with a ratio of 10.41. Total transmission ratio is found as 1:52.05. This reducer input assembly dimensions are suitable to output dimensions of the servo motor. The reducer output hole diameter is 70 mm. Sf of the reducer is 3.94 for 21 kW applications and the reflected inertia is 0.0096 kg m^2 [43].
(11) According to Eq. (15), total system reflected inertia was found as 0.0146 kg m^2 by adding gear box inertia. Then, the inertia ratio was calculated as about 1 by using Eq. (14). This value is under limit ratio and approximates the best value.
(12) RMS torque value was also considered. Since the motion scenario was defined as intermittent duty (S3–S6), RMS torque value was determined by using Eq. (16) from motion profiles as 110 Nm. Since this is lower than RMS torque of the motor (126 Nm), the servo motor selection is done as in Eq. (17).
(13) Reflected motor torque was found by Eq. (13). Efficiency between crank and motor is 92% as there are two reductions with 96% efficiency as shown in Fig. 3. Motor torque and speed were

Table 3 M_2053090 servo motor specifications [42]

Stall		Nominal			Peak		Inertia (kg m^2)
Torque (Nm)	Current (A)	Torque (Nm)	Speed (rpm)	Power (kW)	Torque (Nm)	Speed (rpm)	
90	59	62	3000	18.6	400	3700	0.0145

found by Eq. (12) for speed and Eq. (13) for torque as given in Fig. 6a.

(14) The rated press torque, stroke, and velocity capacity (for 50 tons) can be calculated using the dynamic equations. Servo motor's maximum capacities are 400 Nm of torque and 3700 rpm of velocities on the crank. Considering efficiencies, 50 tons rated force was found at about 7 mm stroke (Fig. 6b) in which motor peak value is about 400 Nm. Maximum ram velocity for 200 mm stroke is found as about 71 spm without load. So the rated load is found at 7 mm stroke, and its maximum velocity is 71 spm.

The new selection methodology considers critic motion, kinematics, dynamics, and CAD design together with a systematic approach special to servo presses. Torque advantages of PMSM (or AC servo motors) have peak torques about five times higher than nominal torque. These motors are chosen for intermittent cycles in servo presses. The considerations and methodology are approved with the experimental studies.

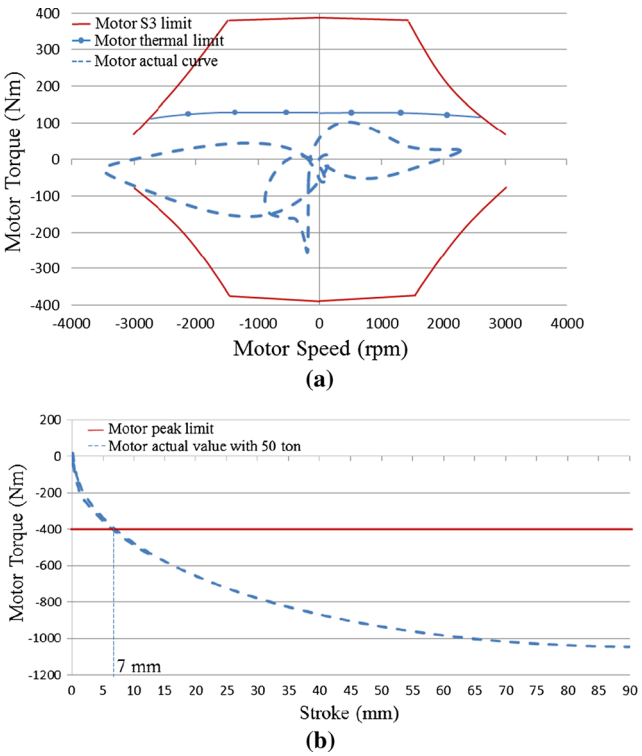

Fig. 6 **a** Motor speed-torque locus and **b** stroke capacity in motor torque (for 50 tons loading)

7 Experimental results

Experimental setup includes the following parts: multi-touch control panel, I/O terminals, servo driver, servo motor, motor position encoder, gearbox, servo press mechanism and body, linear encoder, and safety barriers. TwinCAT® software scope saves the experimental results during system operation. Motion automation is performed by TwinCAT®-PLC [44]. It offers an integrated system with software and hardware. Figure 7 shows the prototype is manufactured. Selected or generated motion is defined by using the multi-touch control panel, and the servo driver is acted by signals via I/O terminals. Classical cascade loop is applied with feed forward. Current feedback is provided compensation for the motor and load inertia. Velocity feedback control is improved velocity characteristics and disturbance ability. Auto-tuning is also performed.

The critic soft motion in Fig. 2 was used for design and motor selection steps. Having manufactured the servo crank press, soft motion is revised to get better precision by using by using TwinCat/CAM Design Tool®. Many experiments are applied under free reaction force. Figure 8a gives final form of the soft motion performance. Here, the command and the responses term indicate the input parameter and experimental results of the ram position. The result is compared and high machine position accuracy is observed. The touch time of scenarios about BDC has following error which is smaller than 0.025 mm. The dynamic modeling was used design and motor selection steps. Motor torque results are shown in Fig. 8b. The theoretical torque and the experimental torque results are given. Calculated value indicates the numeric motor torque results by Eqs. (7) and (13). The experimental result indicates the experimental torque reading.

8 Conclusions

Four main issues are presented in this study for a servo press: system dynamic model, 3D CAD design, servo motor selection, and the experimental study. The significant results in the study are given below:

- Dynamic modeling and simulation were performed by using the real values of press with soft motion ram scenario.
- A new methodology for servo motor and gear box selection was presented. An optimum servo motor selection was performed. Thus, cost of the servo press manufacturing is reduced.

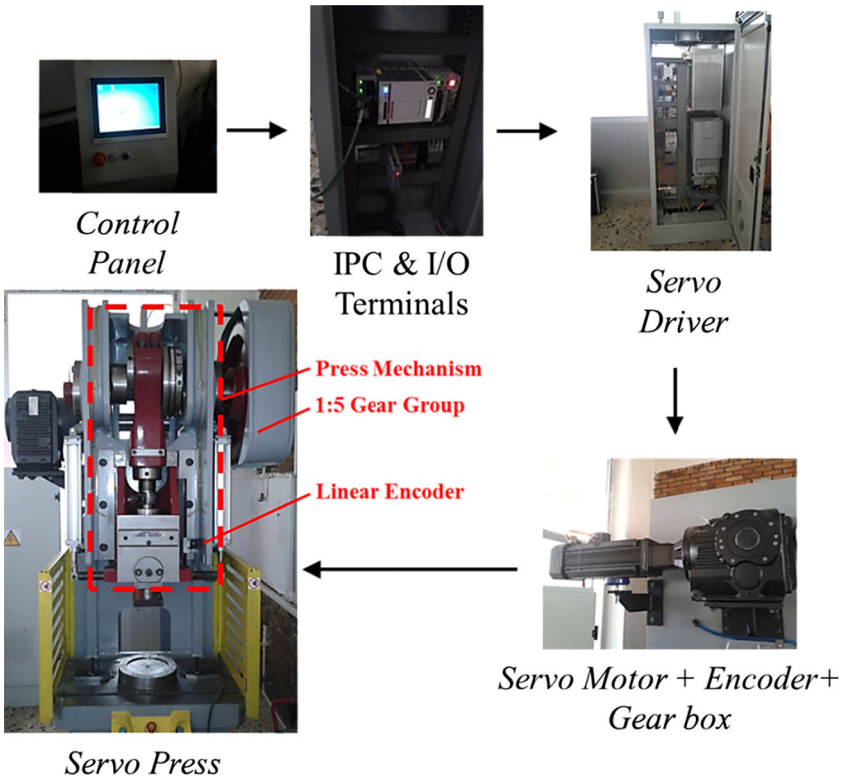

Fig. 7 Servo press experimental setup

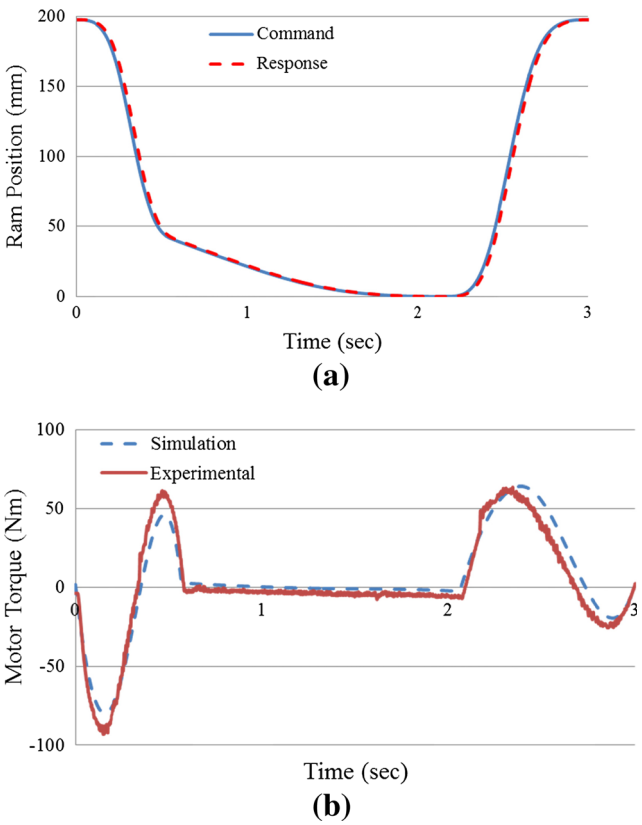

Fig. 8 **a** Experimental ram stroke result (soft motion) and **b** motor torque experimental validation

- Rated values were determined for servo crank press with 50 tons and 200 mm stroke capacity. PMSM servo motor with nominal 62 Nm and 3000 rpm (18.6 kW) was selected. Motor simulation results are presented. The motor is provided the soft motion concept with rated load of 50 tons about 7 mm stroke. The press's ram speed capacity of 71 spm for 200 mm stroke.
- The press is manufactured, and the experimental study is applied. A critical motion is selected and implemented. The mathematical model is validated by finding acceptable results for motion following accuracy. The manufacturing accuracy is observed as ±0.025 mm which is acceptably good accuracy for a servo mechanical press.
- The same capacity presses are compared in industry [45]. According to the selected motor capacity, the manufactured servo press has provided higher performance capacity. The manufactured press has given higher rated tonnage point, higher stroke capacity and higher speed (relative stroke) compared with the available ones.

Compliance with ethical standards

Funding This work was supported by the Ministry of Science, Industry and Technology under SANTEZ project (01422.STZ.2012-I), Turkey.

Appendix

All of the dynamic point's kinematics, i.e., position, velocities, and accelerations are necessary for the dynamic analysis. Geometrically, positions of the centers can be written as Eqs. (22–24). First and second derivatives of the equations are used for Lagrange approach.

$$x_{cg1} = r^{'}\sin\theta, \qquad y_{cg1} = -r^{'}\cos\theta \tag{22}$$

$$x_{cg2} = \left(l-l^{'}\right)\sin\beta, \qquad y_{cg2} = -(r\cos\theta + l^{'}\cos\beta) \tag{23}$$

$$x_3 = 0, \qquad y_3 = -(r\cos\theta + l\cos\beta) \tag{24}$$

$$\dot{\beta} = \frac{r\cos\theta\dot{\theta}}{\sqrt{l^2-r^2\sin^2\theta}} = c\dot{\theta} \tag{25}$$

System work equation is given by Eq. (26). By using Eq. (26), equations are written for external forces as Eq. (27).

$$\delta W = \tau\delta\theta + F\delta y_3 = \tau\delta\theta + F(r\sin\theta\delta\theta + l\sin\beta\delta\beta) \tag{26}$$

$$Q_k = \frac{\delta W}{\delta\theta} = \tau + Fr\sin\theta(1+c) \tag{27}$$

Kinetic and potential energy equations are given in Eqs. (28–29). T is total kinetic energy, and V is total potential energy. Mechanism parameters are m_1, m_2, and m_3 are masses of the crank, the rod, and the ram, respectively, I_1 and I_2 are inertias of crank and rod, respectively.

$$T = \frac{1}{2}r^2\dot{\theta}^2\left(\frac{I_1 + I_2c^2 + m_1r'^2}{r^2} + \frac{\left(l-l^{'}\right)^2}{l^2}m_2\cos^2\theta + \sin^2\theta\left(\frac{l'^2}{l^2}m_2c^2 + 2\frac{l^{'}}{l}m_2c + m_3c^2 + 2m_3c + m_2 + m_3\right)\right) \tag{28}$$

$$V = -g\cos\theta\left(m_1r^{'} + m_2r + m_3r\right) - g\sqrt{l^2-r^2\sin^2\theta}\left(\frac{l^{'}}{l}m_2 + m_3\right) \tag{29}$$

Equations (28) and (29) are substituted in Eq. (5) and Lagrange function is found as Eq. (30) where the generalized coordinate, θ is written. Equation (27) is substituted in Eq. (6), and Eq. (31) is then written.

$$L = \frac{1}{2}r^2\dot{\theta}^2\left(\frac{I_1 + I_2c^2 + m_1r'^2}{r^2} + \frac{\left(l-l^{'}\right)^2}{l^2}m_2\cos^2\theta + \sin^2\theta\left(\frac{l^{'2}}{l^2}m_2c^2 + 2\frac{l^{'}}{l}m_2c + m_3c^2 + 2m_3c + m_2 + m_3\right)\right) + g\cos\theta\left(m_1r^{'} + m_2r + m_3r\right) + g\sqrt{l^2-r^2\sin^2\theta}\left(\frac{l^{'}}{l}m_2 + m_3\right) \tag{30}$$

$$\frac{\mathrm{d}}{\mathrm{d}t}\left(\frac{\mathrm{d}L}{\mathrm{d}\dot{\theta}}\right) - \frac{\mathrm{d}L}{\mathrm{d}\theta} = Q_k = \tau + Fr\sin\theta(1+c) \tag{31}$$

After Lagrange function (in which the generalized coordinate θ is written) is determined, partial derivations of Lagrange equation can be given as Eqs. (32–34).

$$\frac{\mathrm{d}L}{\mathrm{d}\dot{\theta}} = \dot{\theta}r^2\left(\frac{I_1 + I_2c^2 + m_1r'^2}{r^2} + \frac{\left(l-l^{'}\right)^2}{l^2}m_2cos^2\theta + sin^2\theta\left(\frac{l^{'2}}{l^2}m_2c^2 + 2\frac{l^{'}}{l}m_2c + m_3c^2 + 2m_3c + m_2 + m_3\right)\right) \tag{32}$$

$$\frac{\mathrm{d}}{\mathrm{d}t}\left(\frac{\mathrm{d}L}{\mathrm{d}\dot{\theta}}\right)=\ddot{\theta}r^2\left(\frac{I_1+I_2c^2+m_1r'^2}{r^2}+\frac{\left(l-l'\right)^2}{l^2}m_2\cos^2\theta+\sin^2\theta\left(\frac{l'^2}{l^2}m_2c^2+2\frac{l'}{l}m_2c+m_3c^2+2m_3c+m_2+m_3\right)\right)$$
$$+\dot{\theta}r^2\left(2\sin^2\theta\frac{\sin\theta}{\cos\theta}\dot{\theta}\left(c^3-c\right)\left(c\left(\frac{I_2}{r^2\sin^2\theta}+\frac{l'^2}{l^2}m_2+m_3\right)+\frac{l'}{l}m_2+m_3\right)+2\sin\theta\cos\theta\dot{\theta}\left(-\frac{\left(l-l'\right)^2}{l^2}m_2+c^2\left(\frac{l'^2}{l^2}m_2+m_3\right)+2c\left(\frac{l'}{l}m_2+m_3\right)+m_2+m_3\right)\right) \tag{33}$$

$$\frac{dL}{d\theta}=\frac{1}{2}\dot{\theta}r^2\left(2\sin^2\theta\frac{\sin\theta}{\cos\theta}\dot{\theta}\left(c^3-c\right)\left(c\left(\frac{I_2}{r^2\sin^2\theta}+\frac{l'^2}{l^2}m_2+\mathrm{m}_3\right)+\frac{l'}{l}m_2+m_3\right)+2\sin\theta\cos\theta\dot{\theta}\left(-\frac{\left(l-l'\right)^2}{l^2}m_2+c^2\left(\frac{l'^2}{l^2}m_2+m_3\right)+2c\left(\frac{l'}{l}m_2+m_3\right)+m_2+m_3\right)\right)$$
$$-gr\sin\theta\left(\frac{r'}{r}m_1+\frac{l'}{l}m_2c+m_3c+m_2+m_3\right) \tag{34}$$

These partial derivations are substituted in their places as Eq. (31). Then Eq. (7) is resulted as system dynamic model.

References

1. Osakada K, Mori K, Altan T, Groche P (2011) Mechanical servo press technology for metal forming. CIRP Ann Manuf Technol 60(2):651–672. doi:10.1016/j.cirp.2011.05.007
2. Hayashi H, Nishimura H (2009) The application of servo press machine to forming of sheet metals with low formability. The Annals of "Dunarea De Jos" University of Galati Fascicle V, Technologies in Machine Building, ISSN1221-4566
3. Halicioglu R, L.C. D (2013) Krank Pres Mekanizması: Kinematik Analizi ve Benzetimi. Paper presented at the UMTS, Erzurum
4. Halicioglu R, Dulger LC, Bozdana AT (2014) Modelling and simulation based on MATLAB/Simulink: a press mechanism. Paper presented at the Journal of Physics: Conference Series
5. Halicioglu R, Dulger LC, Bozdana AT (2016) Mechanisms, classifications, and applications of servo presses: a review with comparisons. Proceedings of the institution of mechanical engineers. part B. Journal of Engineering Manufacture 230(7):1177–1194. doi:10.1177/0954405415600013
6. Qingyu S, Baofeng G, Jian L (2013) Drawing motion profile planning and optimizing for heavy servo press. Int J Adv Manuf Technol 69(9–12):2819–2831
7. Fung RF, Chen KW (1998) Dynamic analysis and vibration control of a flexible slider–crank mechanism using PM synchronous servo motor drive. J Sound Vib 214(4):605–637. doi:10.1006/jsvi.1998.1556
8. Ha J-L, Fung R-F, Chen K-Y, Hsien S-C (2006) Dynamic modeling and identification of a slider-crank mechanism. J Sound Vib 289(4):1019–1044
9. Bai J, Tong S, Yu Z, Zheng D (2010) Analysis and simulations of inertia force in ultra high speed stamping machine. Journal of Networks 5(12):1475–1480
10. He K, Li W, Du R (2006) Dynamic modelling with kineto-static method and experiment validation of a novel controllable mechanical metal forming press. Int J Manuf Res 1(3):354–378
11. Li H, Zhang Y, Zheng H (2008) Dynamics modeling and simulation of a new nine-bar press with hybrid-driven mechanism. J Mech Sci Technol 22(12):2436–2444
12. Li H, Zhang Y (2010) Seven-bar mechanical press with hybrid-driven mechanism for deep drawing; part 1: kinematics analysis and optimum design. J Mech Sci Technol 24(11):2153–2160
13. Jun L (2006) A study of the dynamic of slider-crank mechanism. Journal of Shanghai Dianji University 9(4):24–28
14. Xingguo M, Xiaomei Y, Bangchun W (2007) Multi-body dynamics simulation on flexible crankshaft system. In: Proceeding of the 12th IFToMM World Congress, Besancon, France, 18th–21st June 2007
15. Liu, M, Cao, Y, Zhang, Q, Zhou, H (2010) Kinematics and dynamics simulation of the slider-crank mechanism based on MATLAB/Simulink. In: Computer Application and System Modeling (ICCASM), International Conference on 2010:V9–557-V559–563. IEEE
16. Daniel GB, Cavalca KL (2011) Analysis of the dynamics of a slider–crank mechanism with hydrodynamic lubrication in the connecting rod–slider joint clearance. Mech Mach Theory 46(10):1434–1452. doi:10.1016/j.mechmachtheory.2011.05.007
17. Abdullah MN, Telegin VV (2011) Modeling of dynamic processes of the main executive mechanism of the hot-crank press. Al-Rafadain Engineering Journal 19(4):1–10

18. Anis A (2012) Simulation of slider crank mechanism using ADAMS software. International Journal of Engineering & Technology 12(4):108–112
19. Endou J (2008) Innovation of press working by servo press. Journal-Japan Society for Technology of Plasticity 49(2):4
20. Aida (2012) Catalog Of Aida; AIDA Direct Servo Formers DSF-N1 and N2 Series. In: Web; http://www.aida.co.jp/en/products/product12.html
21. Siemens, AG (2008) Spectrum metal forming. pp. 12–17
22. Coskunoz (2012) Coskunoz metal form. Bursa/Turkey
23. Karakoc (2014) KLP Machine Group Press Catalog
24. Baumueller (2014) DST2 high torque servo motors catalog. Nürnberg
25. Amada Catalog of AE-NT and EM-NT series. Amada America Inc
26. Amada (2010) Catalog of SDE series. Amada GMBH, Germany
27. Seyi (2012) Catalog of SD1-SD2 series. Seyi Europe GmbH
28. Komatsu (2013) Catalog of H1F-H2W series. Komatsu America Industries LLC, Ilinois
29. Kütük ME (2013) Hybrid machine systems: analysis and control. Msc, Gaziantep University
30. Ginsberg J (2008) Engineering dynamics, vol. 10. Cambridge University Press
31. Halicioglu R, Dulger LC, Bozdana AT (2016) Structural design and analysis of a servo crank press. Engineering Science and Technology, an International Journal 19(4):2060–2072. doi:10.1016/j.jestch.2016.08.008
32. Bulatović ŽM, Tomić M, Knežević D, Cvetić M (2011) Evaluation of variable mass moment of inertia of the piston–crank mechanism of an internal combustion engine. Proceedings of the Institution of Mechanical Engineers, part D. Journal of Automobile Engineering 225(5):687–702
33. Kissell, TE (2003) Industrial electronics: applications for programmable controllers, instrumentation and process control, and electrical machines and motor controls. Prentice Hall
34. Boerger D (2003) Servo technology meets mechanical presses. Stamping Journal:32
35. Parker (1997) ZX/ZXF Indexer Drive User Guide. Compumotor Division Parker Hannifin Corporation
36. GEIndustrialSystems hand book: AC Motor Selection and Application Guide, vol. GET-6812C. Indiana
37. Mazurkiewicz J (2002) Load inertia and motor selection. Motion Control Association
38. Cetinkunt S (2007) Mechatronics. Wiley, USA
39. Roos F, Johansson H, Wikander J (2006) Optimal selection of motor and gearhead in mechatronic applications. Mechatronics 16(1): 63–72
40. Budimir M, Meyer S (2014) Motor selection & gearbox matching. Groschopp-TechTips. http://s3.amazonaws.com/2013_pdfs/Groschopp/Groschopp-Tech-Tip.pdf
41. SEW (2002) Product catalog of SEW eurodrive: varigear variable speed drives. vol. 9PD0008/2002. Sew-Eurodrive Inc., USA
42. Parker (2012) Parker MB/MH Series Servo Motors Catalog. Parker Hannifin Corporation
43. SEW-eurodrive (2009) Servo gear units of SEW catalog and webside. SEW eurodrive-driving the world, Bruchsal/Germany
44. Beckhoff. http://www.beckhoff.com.tr/english.asp?twincat/. Accessed 29 June
45. Halicioglu R (2015) Design, synthesis and control of a mechanical servo press: an industrial application. PhD, Gaziantep University